Four-dimensional optical multiband-OFDM for beyond 1.4 Tb/s serial optical transmission

Ivan Djordjevic,[1,*] Hussam G. Batshon,[1] Lei Xu,[2] and Ting Wang[2]

[1]*University of Arizona, Depart. Electrical & Computer Eng., 1230 E. Speedway Blvd., Tucson, AZ 85721, USA*
[2]*NEC Laboratories America, 4 Independence Way, Princeton, NJ 08540, USA*
**ivan@ece.arizona.edu*

Abstract: We propose a four-dimensional (4D) coded multiband-OFDM scheme suitable for beyond 1.4 Tb/s serial optical transport. The proposed scheme organizes the *N*-dimensional (*N*D) signal constellation points in the form of signal matrix; employs 2D-inverse FFT and 2D-FFT to perform modulation and demodulation, respectively; and exploits both orthogonal polarizations. This scheme can fully exploit advantages of OFDM to deal with chromatic dispersion, PMD and PDL effects; and multidimensional signal constellations to improve OSNR sensitivity of conventional optical OFDM. The improvement of 4D-OFDM over corresponding polarization-multiplexed QAM (with the same number of constellation points) ranges from 1.79 dB for 16 signal constellation point-four-dimensional-OFDM (16-4D-OFDM) up to 4.53 dB for 128-4D-OFDM.

OCIS codes: (060.0060) Fiber optics and optical communications; (060.4080) Modulation; (999.9999) Orthogonal frequency division multiplexing; (OFDM); (999.9999) Low-density parity-check; (LDPC) codes; (999.9999) Multidimensional signal constellations.

References and links

1. J. Hong, and T. Schmidt, "40G and 100G modules enable next generation networks," in Proc. SPIE, Communications and Photonics Conference and Exhibition 2009 (ACP 2009) **7631**, 763115 (2009).
2. H. G. Batshon, I. B. Djordjevic, L. Xu, and T. Wang, "Modified hybrid subcarrier/amplitude/ phase/polarization LDPC-coded modulation for 400 Gb/s optical transmission and beyond," Opt. Express **18**(13), 14108–14113 (2010).
3. H. G. Batshon, I. B. Djordjevic, L. Xu, and T. Wang, "Multidimensional LDPC-coded modulation for beyond 400 Gb/s per wavelength transmission," IEEE Photon. Technol. Lett. **21**(16), 1139–1141 (2009).
4. H. G. Batshon, I. B. Djordjevic, and T. Schmidt, "Ultra high speed optical transmission using subcarrier-multiplexed four-dimensional LDPC-coded modulation," Opt. Express **18**(19), 20546–20551 (2010).
5. L. J. Stankovic, *Digital Signal Processing* (Naucna Knjiga, 1990).
6. C. Chakrabarti, and J. JaJa, "VLSI architectures for multidimensional transforms," IEEE Trans. Comput. **40**(9), 1053–1057 (1991).
7. W. Shieh, and I. Djordjevic, *OFDM for Optical Communications* (Elsevier/Academic Press, 2009).
8. I. B. Djordjevic, M. Arabaci, and L. Minkov, "Next generation FEC for high-capacity communication in optical transport networks," J. Lightwave Technol. **27**(16), 3518–3530 (2009).
9. J. McDonough, "Moving standards to 100 GbE and beyond," IEEE Appl. Pract. **45**, 6–9 (2007).
10. Y. Ma, Q. Yang, Y. Tang, S. Chen, and W. Shieh, "1-Tb/s single-channel coherent optical OFDM transmission over 600-km SSMF fiber with subwavelength bandwidth access," Opt. Express **17**(11), 9421–9427 (2009).
11. Y. Tang, and W. Shieh, "Coherent optical OFDM transmission up to 1 Tb/s per channel," J. Lightwave Technol. **27**(16), 3511–3517 (2009).
12. R. Nagarajan, C. H. Joyner, R. P. Schneider, J. S. Bostak, T. Butrie, A. G. Dentai, V. G. Dominic, P. W. Evans, M. Kato, M. Kauffman, D. J. H. Lambert, S. K. Mathis, A. Mathur, R. H. Miles, M. L. Mitchell, M. J. Missey, S. Murthy, A. C. Nilsson, F. H. Peters, S. C. Pennypacker, J. L. Pleumeekers, R. A. Salvatore, R. K. Schlenker, R. B. Taylor, Huan-Shang Tsai, M. F. Van Leeuwen, J. Webjorn, M. Ziari, D. Perkins, J. Singh, S. G. Grubb, M. S. Reffle, D. G. Mehuys, F. A. Kish, and D. F. Welch, "Large-scale photonic integrated circuits," IEEE J. Sel. Top. Quantum Electron. **11**(1), 50–65 (2005).
13. R. van Nee, and R. Prasad, *OFDM for Wireless Multimedia Communications* (Artech House, 2000).
14. J. G. Proakis, *Digital Communications* (McGraw-Hill, 2001).

1. Introduction

The optical communication systems have been evolving rapidly in recent years in order to adapt to the continuously increasing demand on transmission capacity, coming mainly from

#137646 - $15.00 USD Received 3 Nov 2010; revised 23 Dec 2010; accepted 24 Dec 2010; published 6 Jan 2011

the growing popularity of the Internet and multimedia in everyday life. In order to keep the system complexity reasonably low, the new optical communications solutions have to offer affordable upgrades of currently available optical communication systems operating at lower speeds to satisfy the required higher speeds [1]. One such approach was based on multidimensional coded modulation [2–4]. Namely, by increasing the number of dimensions (i.e., the number of orthonormal basis functions), we can increase the aggregate data rate of the system without degrading the bit error rate (BER) performance as long as orthogonality among basis functions is preserved. Most of the papers on multidimensional signal constellations for optical communications so far have been related to single carrier systems.

In this paper, which can be considered as generalization of [4], we describe how to map multidimensional signal constellation points in coherent optical orthogonal frequency division multiplexing (OFDM) systems. The key idea is to exploit all advantages of both of OFDM and multidimensional single carrier systems. The multidimensional mapper for OFDM can be described as follows. Let N-dimensional signal constellation point be represented as $\boldsymbol{S} = (S^{(0)},S^{(1)},\ldots,S^{(N-1)})$, where $S^{(l)}$ ($l = 0,\ldots,N-1$) is the lth coordinate. Let the duration of the signal frame be M signal constellation points. We can represent the signal constellation points in matrix form, by placing the coordinates of signal constellation points along the columns of a signal matrix. We further apply two-dimensional inverse fast Fourier transform (2D-IFFT) to obtain 2D-IFFT array of complex numbers. The coordinates of complex numbers can be considered as in-phase (I) and quadrature (Q) channels, while even and odd rows of two-dimensional array can be mapped to x- and y-polarizations, respectively. The arbitrary N-dimensional ($N = 2,3,4,5,\ldots$) signal constellation can be used in combination with this scheme. Because in optical channel we have four bases functions (in-phase, quadrature, x-polarization and y-polarization) available, the full advantage of this scheme can be obtained by employing the 4D signal constellations. All other steps of this 2D-OFDM scheme are similar to conventional coherent optical OFDM. On receiver side, we use the conventional polarization-diversity receiver, followed by 2D-FFT demapper. Therefore, this scheme can fully exploit the advantages of OFDM as an efficient way to deal with chromatic dispersion, polarization mode dispersion (PMD) and polarization dependent loss (PDL) effects. At the same time we can exploit the advantages of multidimensional signal constellation to improve the optical signal-to-noise ratio (OSNR) sensitivity of conventional optical OFDM dramatically. We also describe a 4D coherent optical multiband-OFDM scheme enabling 1.4 Tb/s serial optical transmission.

The paper is organized as follows. The proposed 4D low-density parity-check (LDPC)-coded OFDM is described in Section 2. In Section 3, we describe the 4D multiband-OFDM as a beyond 1 Tb/s serial optical transport enabling technology. The performance analysis results are provided in Section 4. Finally, some important concluding remarks are given in Section 5.

2. Description of 4D coded optical OFDM

The proposed 4D LDPC-coded optical OFDM system is shown in Fig. 1. The m independent data streams are encoded using different LDPC (n,k_l) codes ($l = 1,\ldots,m$), where n denotes the codeword length and k_l is the information word length of lth component code. The codewords are written row-wise into $m \times n$ bit interleaver. The m bits are taken from bit interleaver column-wise at every symbol slot i and are used as input of 4D mapper, which selects one constellation point out of 2^m, depending on information content. The 4D mapper is implemented as a look-up table (LUT) with m input bits serving as a memory address that selects the four coordinates of 4D signal constellation point. The outputs of 4D mapper are written column-wise into $4 \times M$ symbol-like interleaver. The content of symbol interleaver can be represented as a two-dimensional array (matrix) as follows:

#137646 - $15.00 USD Received 3 Nov 2010; revised 23 Dec 2010; accepted 24 Dec 2010; published 6 Jan 2011

$$S\left(\vec{k}\right)=\left[S\left(k_1,k_2\right)\right]_{4\times M}=\begin{bmatrix} S_{00} & S_{10} & \cdots & S_{M-1,0} \\ S_{01} & S_{11} & \cdots & S_{M-1,1} \\ S_{02} & S_{12} & \cdots & S_{M-1,2} \\ S_{03} & S_{13} & \cdots & S_{M-1,3} \end{bmatrix}, \quad (1)$$

where the jth column $\boldsymbol{S}_j = [S_{j,0}\ S_{j,1}\ S_{j,2}\ S_{j,3}]^{\mathrm{T}}$ represents the coordinates of jth 4D signal constellation point $(S_j^{(0)},S_j^{(1)},S_j^{(2)},S_j^{(3)})$ (j = 0,1,…,M-1). Therefore, the rows correspond to the dimensions and columns to subcarriers. Notice that conventional PolMux OFDM requires 2 × 2M signaling matrix for the same amount of data, and the bandwidth requirements are therefore identical. This two-dimensional array is used as input to the two-dimensional inverse discrete Fourier transform (2D-IDFT) block, which calculates the IDFT as follows

$$s\left(\vec{n}\right)=\sum_{k_1=0}^{M-1}\sum_{k_2=0}^{M-1}X\left(\vec{k}\right)e^{j\vec{n}\vec{k}2\pi/M},\ \vec{k}=\left[k_1\ k_2\right]^T,\ \vec{n}=\left[n_1\ n_2\right]^T \quad (2)$$

where $X\left(\vec{k}\right)$ is obtained by concatenating M/4 sub-matrix blocks of type (1), so that the duration of signal per axis is M. In Eq. (2), we use $\vec{n}\vec{k}$ to denote dot product of $\vec{n}=\left[n_1\ n_2\right]^T$ and $\vec{k}=\left[k_1\ k_2\right]^T$ as follows $\vec{n}\vec{k}=n_1k_1+n_2k_2$. The result of 2D-IDFT block is 2D array of complex numbers:

$$s\left(\vec{n}\right)=\left[s\left(n_1,n_2\right)\right]_{M\times M}=\begin{bmatrix} s_{00} & s_{10} & \cdots & s_{M-1,0} \\ s_{01} & s_{11} & \cdots & s_{M-1,1} \\ \vdots & \vdots & \cdots & \vdots \\ s_{0,M-1} & s_{1,M-1} & \cdots & s_{M-1,M-1} \end{bmatrix}, \quad (3)$$

where s_{ij} = ($s_{ij,\mathrm{I}}$, $s_{ij,\mathrm{Q}}$), with subscripts I and Q corresponding to in-phase and quadrature channels, respectively. More details on multidimensional DFT can be found in [5], and for VLSI implementation an interested reader is referred to [6]. The matrix (3) is further serialized into two vector-streams $\vec{x}=\left[s_{00}\,s_{10}\cdots s_{M-1,0}\ s_{02}\,s_{12}\cdots s_{M-1,2}\cdots\right]$ and $\vec{y}=\left[s_{01}\,s_{11}\cdots s_{M-1,1}\ s_{03}\,s_{13}\cdots s_{M-1,3}\cdots\right]$. The row-vector $\vec{x}$ is obtained by concatenating even rows in Eq. (3), while the row-vector $\vec{y}$ is obtained by concatenating the odd rows in Eq. (3). The elements of row-vector $\vec{x}$ (row-vector $\vec{y}$), namely $s_{\mathrm{x},i}$ = ($I_{\mathrm{x},i}$ $Q_{\mathrm{x},i}$) [$s_{\mathrm{y},i}$ = ($I_{\mathrm{y},i}$ $Q_{\mathrm{y},i}$)], corresponding to x- (y-) polarization, are used (after digital-to-analog (D/A) conversion) as inputs to the I/Q modulator as shown in Fig. 2(b) of reference [4]. Alternatively, the polar modulator shown in Fig. 1(c) can be used. The corresponding streams in x- and y-polarizations are multiplexed in polarization beam combiner (PBC) as shown in Fig. 1(c) and transmitted over the optical transmission system of interest. Notice that arbitrary N-dimensional (N = 2,3,4,5,…) signal constellation can be used. Because in optical channel we have four bases functions available, the full advantage of this scheme can be obtained by employing the 4D signal constellations. (The cyclic extension insertion principle and A/D conversion operation are very similar to that in conventional OFDM and as such are not discussed here.)

At the receiver side, and using the polarization beam splitter (PBS), the optical signal is split into two orthogonal polarizations that are used as input into two balanced coherent detectors. The balanced coherent detectors provide the estimated in-phase and quadrature information for both polarizations. The outputs of the balanced detectors, after A/D conversion, cyclic extension removal and carrier recovery, are processed by 2D-DFT block.

#137646 - $15.00 USD Received 3 Nov 2010; revised 23 Dec 2010; accepted 24 Dec 2010; published 6 Jan 2011

Notice that both 2D-IDFT and 2D-DFT can be efficiently calculated based on 2D fast Fourier transform (2D-FFT) algorithm. The simplest 2D-FFT algorithm is based on one-dimensional FFT and requires $2M \times M\log_2 M$ complex multiplications and additions. The complexity of this algorithm is $M^4/[2M^2\log_2 M]$ times lower than that of direct 2D-DFT computation. Upon the deinterleaving, the symbol log-likelihood ratios (LLRs) are calculated in the *a posteriori* probability (APP) demapper using the following equation,

$$\lambda(S_i) = \log\left[P(S_0|R_i)/P(S_i|R_i)\right], \tag{4}$$

where $P(\mathrm{S}_i|\mathrm{R}_i)$ is determined by Bayes' rule as:

$$P(S_i|R_i) = P(R_i|S_i)P(S_i)\Big/\sum_{S'} P(R_i|S_i')P(S_i'). \tag{5}$$

By substituting Eq. (5) into Eq. (4) we obtain:

$$\lambda(\mathrm{S}_i) = \log\left[\frac{P(\mathrm{R}_i|\mathrm{S}_i)P(\mathrm{S}_i)}{P(\mathrm{R}_i|\mathrm{S}_0)P(\mathrm{S}_0)}\right] = \log\left[\frac{P(\mathrm{R}_i|\mathrm{S}_i)}{P(\mathrm{R}_i|\mathrm{S}_0)}\right] + \log\left[\frac{P(\mathrm{S}_i)}{P(\mathrm{S}_0)}\right] = \log\left[\frac{P(\mathrm{R}_i|\mathrm{S}_i)}{P(\mathrm{R}_i|\mathrm{S}_0)}\right] + \lambda_a(\mathrm{S}_i), \tag{6}$$

where $\lambda_a(\mathrm{S}_i) = \log\left[P(\mathrm{S}_i)/P(\mathrm{S}_0)\right]$ is the prior symbol LLR, which can be calculated by:

$$\lambda_a(\hat{\boldsymbol{s}}) = \sum_{j=1}^{m} c_j L_{D,e}(c_j), \tag{7}$$

where

$$L_{D,e}(\hat{c}_j) = L\left(c_j^{(t)}\right) - L\left(c_j^{(t-1)}\right), \tag{8}$$

and c_j denotes the jth bit in the observed symbol $\boldsymbol{S}$ binary representation $\boldsymbol{c} = (c_0,c_1,\ldots)$. In Eq. (8), we use $L(c^{(t)}_j)$ to denote the LDPC decoder output in current iteration (iteration t). In the above equations $\boldsymbol{S}_i = \left[S_i^{(0)}\ S_i^{(1)}\ S_i^{(2)}\ S_i^{(3)}\right]^T$ denotes the transmitted signal constellation point, $\boldsymbol{R}_i$ denotes the received constellation point, and $\boldsymbol{S}_0$ denotes the referent constellation point. The $P(\boldsymbol{R}_i|\boldsymbol{S}_i)$, from Eq. (6), denotes the conditional probability that can be estimated by collection of histograms. The bit LLRs $L(c_j)$ are determined from symbol LLRs by

$$L(\hat{c}_j) = \log\frac{\sum_{\boldsymbol{c}:c_j=0}\exp\left[\lambda(\boldsymbol{S})\right]\exp\left(\sum_{\boldsymbol{c}:c_k=0,k\neq j} L_a(c_k)\right)}{\sum_{\boldsymbol{c}:c_j=1}\exp\left[\lambda(\boldsymbol{S})\right]\exp\left(\sum_{\boldsymbol{c}:c_k=0,k\neq j} L_a(c_k)\right)}. \tag{9}$$

Therefore, the jth bit reliability is calculated as the logarithm of the ratio of a probability that $c_j = 0$ and probability that $c_j = 1$. In the nominator, the summation is done over all symbols $\boldsymbol{S}$ having 0 at the position j, while in the denominator over all symbols $\boldsymbol{S}$ having 1 at the position j. With $L_a(c_k)$ we denoted the prior (extrinsic) information determined from the APP demapper. The inner summation in Eq. (9) is performed over all bits of symbol $\boldsymbol{S}$, selected in the outer summation, for which $c_k = 0$, $k\neq j$. The bit LLRs are forwarded to LDPC decoders, which provide extrinsic bit LLRs for demapper according to Eqs. (8) and (7), and are used as inputs to Eq. (6) as the prior information based on Eq. (7).

#137646 - $15.00 USD Received 3 Nov 2010; revised 23 Dec 2010; accepted 24 Dec 2010; published 6 Jan 2011

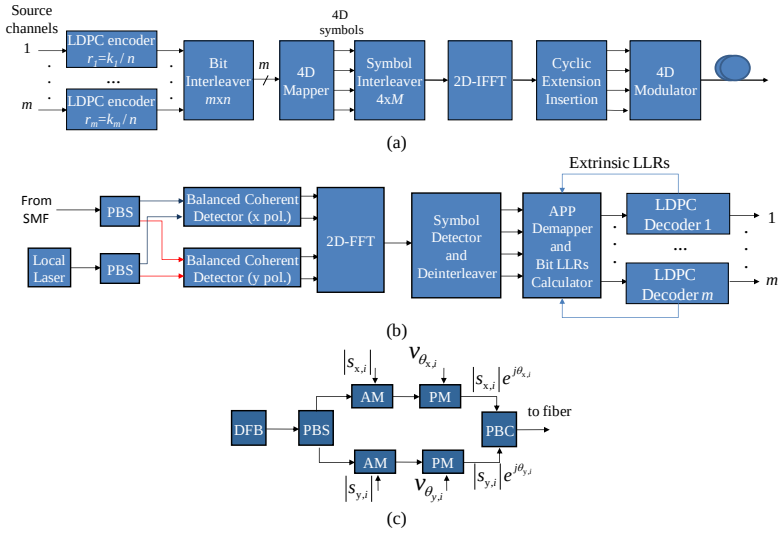

Fig. 1. Proposed 4D LDPC-coded OFDM scheme: (a) Tx and (b) Rx configurations. (c) The 4D modulator configuration in polar (amplitude/phase) coordinates. PBS/C: polarization beam splitter/combiner, 3 dB: 3 dB coupler, MAP: maximum *a posteriori* probability, LLRs: log-likelihood ratios.

Similarly as in conventional coherent optical OFDM systems in quasi-linear regime, the received 4D symbol vector of kth subcarrier in ith OFDM symbol $\boldsymbol{R}_{i,k} = [R^{(0)}_{i,k}\ R^{(1)}_{i,k}\ R^{(2)}_{i,k}\ R^{(3)}_{i,k}]^{\mathrm{T}}$ can be represented by

$$\boldsymbol{R}_{i,k} = \boldsymbol{H}_k \boldsymbol{S}_{i,k} e^{j\left[\phi_{\mathrm{CD}}(k)+\phi_{\mathrm{T}}-\phi_{LO}\right]} + \boldsymbol{N}_{i,k}, \qquad (10)$$

where $\boldsymbol{S}_{i,k} = [S^{(0)}_{i,k}\ S^{(1)}_{i,k}\ S^{(2)}_{i,k}\ S^{(3)}_{i,k}]^{\mathrm{T}}$ denotes the transmitted symbol vector of kth subcarrier in ith OFDM symbol. We use superscript (l) to denote the lth (l = 0,1,2,3) coordinate of corresponding signal constellation point. In Eq. (10), $\boldsymbol{N}_{i,k} = [N^{(0)}_{i,k}\ N^{(1)}_{i,k}\ N^{(2)}_{i,k}\ N^{(3)}_{i,k}]^{\mathrm{T}}$ denotes the noise vector dominantly determined by the amplified spontaneous emission (ASE) noise; ϕ_{T} and ϕ_{LO} denote the laser phase noise processes of transmitting and local lasers, $\phi_{\mathrm{CD}}(k)$ denotes the phase distortion of kth subcarrier due to chromatic dispersion, and $\boldsymbol{H}_k$ denotes the channel matrix of kth subcarrier, which is similar to the Jones matrix described in [7,8]. Therefore, the equivalent model of proposed 4D OFDM scheme is similar to that of polarization-multiplexed (PolMux) OFDM, so that similar behavior is expected in terms of chromatic dispersion, PMD and PDL tolerance. As opposed to conventional polarization-multiplexed QAM based OFDM systems that multiplex two independent 2D streams, the proposed scheme is 4D scheme and allows full potential of 4D space to be exploited. For the same symbol energy as in 2D space, in 4D space the Euclidean distance between neighboring constellation points is much larger resulting in much better BER performance. In order words, for the same target BER, the OSNR sensitivity is much better in 4D OFDM as shown in Section 4.

3. Description of 4D optical multiband-OFDM

In order to meet high capacity demands, according to some industry experts, the 1 TbE standard should be available by 2012-2013 [9]. Coherent optical OFDM is one promising pathway towards achieving beyond 1 Tb/s optical transport [10,11]. Initial studies [10,11] indicate that the system Q-factor when multiband OFDM with orthogonal sub-bands is used is low (about 13.2 dB after 1000 km of SMF [11]). Such a low Q-factor represents a very tight margin in terms of 7% overhead for RS(255,239) code, and the use of stronger LDPC codes is advocated in [10,11]. In this section, we describe one potential LDPC-coded multiband 4D-OFDM scheme suitable for beyond 1 Tb/s optical transport.

#137646 - $15.00 USD Received 3 Nov 2010; revised 23 Dec 2010; accepted 24 Dec 2010; published 6 Jan 2011

In Fig. 2, we describe the conceptual diagram for multiplexing/demultiplexing enabling beyond 1 Tb/s Ethernet based on multiband 4D-OFDM. The frame corresponding to 1.4 Tb/s (see Fig. 2(a)) is organized in five OFDM bands, each carrying 280 Gb/s traffic, originating from 128 to 4D-OFDM described in previous section as follows 7 × 0.8 × 50 GS/s. The guard spacing between two neighboring OFDM bands is $\Delta f_G = m\Delta f_{sc}$ (m is a positive integer), where Δf_{sc} is the subcarrier spacing. Because the central frequencies of neighboring OFDM bands are orthogonal to each other, we may simplify the separation of OFDM bands by anti-aliasing filters, as explained in [10,11]. Every particular input data stream to the 4D-OFDM subsystem carries 40 Gb/s traffic. The 40 Gb/s traffic can originate from either 40 GbE or 10 GbE, when we need to perform RF multiplexing of four 10 GbE streams. The proposed multiplexing/demultiplexing scheme is compatible with 10 GbE, 40GbE and 100 GbE. For example, two 100 GbE and two 40 GbE data streams can be used as input to 4D-OFDM block to generate 280 Gb/s Ethernet traffic. Notice that the proposal due to Shieh [10] is not compatible with 40 GbE because it employs the 100 Gb/s data rate as the baseband rate. Another advantage of the proposed multiplexing/demultiplexing architecture is that it is essentially two-layer architecture (see Fig. 2(b)), while PolMux-based OFDM architecture [10,11] is three-layer architecture. Finally, the proposed architecture is based on 4D signal constellations, while that in [10,11] is based on 2D constellations and has much stringent OSNR sensitivity requirements.

In Fig. 2(b), we describe our proposed two-layer integrated circuit hierarchy. The baseband level, at 40 Gb/s, can be straightforwardly implemented in CMOS ASIC technology, and 40 Gb/s signal can originate either from 40 GbE or 10 GbE as we explained above. The baseband layer can also be combination of 40 GbE and 100 GbE data streams as indicated above. The second layer is the photonics layer, which can be implemented in photonic integrated circuit (PIC) technology [12], and simply requires the integration of five-frequency.

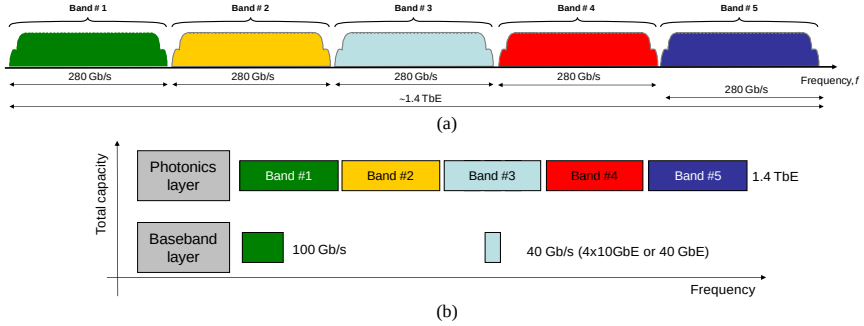

Fig. 2. Conceptual diagram for multiplexing/demultiplexing for 1.4 Tb/s Ethernet: (a) organization of the frame, and (b) the two-layer integrated circuit hierarchy.

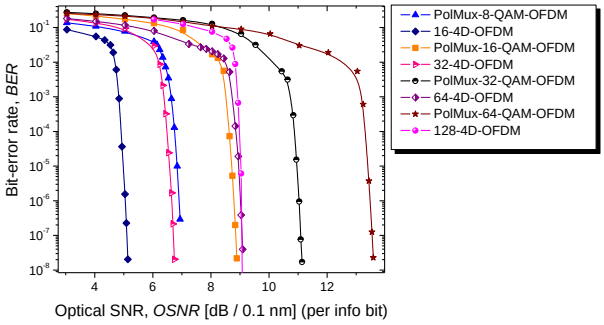

Fig. 3. LDPC-coded 4D-OFDM Band #1 BER performance at baseband information rate of 40 Gb/s.

#137646 - $15.00 USD Received 3 Nov 2010; revised 23 Dec 2010; accepted 24 Dec 2010; published 6 Jan 2011

4. Performance analysis

As an illustration of the potential of the proposed scheme, we show in Fig. 3 the BER performance of the LDPC-coded 4D-OFDM schemes for single-band from Fig. 2. The figure shows the BER performance of single band for different 4D signal constellation sizes for symbol rate of 50 GS/s. In the same figure, we compare the BER performance with conventional PolMux QAM-OFDM. The comparison has been done for the same number of signal constellation points. Notice that because we are concerned with OSNR sensitivity only, the intersymbol interference due to chromatic dispersion and PMD is not observed, so that the BER performance of single-carrier and OFDM systems are the same. This is well known textbook material fact, see for example Fig. 3.2 of [13] (QPSK-OFDM) and Fig. 5.2-16 of [14] (single-carrier QPSK). Namely, the key idea of this paper is to introduce minimum changes in conventional PolMux OFDM and multidimensional single-carrier systems, while fully exploiting the potential of 4D space. The number of subcarriers in both OFDM schemes has been set to 128. For the 16-4D constellation, the signal constellation points are selected by (± 1, ± 1, ± 1, ± 1). For the 32-4D constellation, 16 constellation points are selected by (± ½, ± ½, ± ½, ± ½), 8 as different combinations of (± 1,0,0,0) and its permutations, 4 as (± 1,0,0, ± 1), and the remaining 4 by (0, ± 1, ± 1,0). On the other hand, for the 64-4D constellation, the 64 possible points are mapped to eight of the twelve non-disjoint even permutations of $\frac{1}{2}\left(\pm 1, \pm g_r, \pm \frac{1}{g_r}, 0\right)$, where $g_r = \left(1+\sqrt{5}\right)/2$ is the golden ratio. In addition to signal constellations described above and introduced in [4], we provide a new signal constellation, namely 128-vertices signal constellation. In this signal constellation, 96 vertices are obtained by taking even permutations of ½(± 1, ± g_r, ± 1/g_r,0), and the remaining 32 points are those of the 32-point constellation. We can see that 16-4D-OFDM outperforms PolMux-8-QAM-OFDM by 1.79 dB, 32-4D-OFDM outperforms PolMux-16-QAM-OFDM by 2.14 dB and 64-4D-OFDM outperforms PolMux-32-QAM-OFDM by 2.07 dB, and finally 128-64-4D outperforms PolMux-64-QAM by 4.53dB. The comparison is, therefore, performed for the same number of constellation points.

5. Conclusion

As response to continuously increasing demands on transmission capacity, we proposed the 4D LDPC-coded multiband-OFDM scheme suitable for beyond 1 Tb/s serial optical transport. The proposed scheme is capable of fully exploiting the advantages of both OFDM and multidimensional signal constellation. Signal constellation points are represented in matrix form by placing coordinates of signal constellation points along columns of signal matrix. We further apply 2D inverse FFT to obtain 2D array of complex numbers. Coordinates of complex numbers correspond to I and Q channels, while even and odd rows of 2D array correspond to x- and y-polarizations, respectively. On receiver side, we use conventional polarization-diversity receiver, followed by 2D-FFT demapper. The simulations results indicate that 16-4D-OFDM outperforms PolMux-8-QAM-OFDM by 1.79 dB, 32-4D-OFDM outperforms PolMux-16-QAM-OFDM by 2.14 dB, 64-4D-OFDM outperforms PolMux-32-QAM-OFDM by 2.07 dB, and 128-4D-OFDM outperforms PolMux-64-QAM by 4.53 dB. Therefore, the proposed scheme can fully exploit advantages of OFDM, to deal with chromatic dispersion, PMD and PDL effects; and multidimensional signal constellations to improve significantly the OSNR sensitivity of conventional optical OFDM systems. We also described the multiband 4D-OFDM scheme enabling 1.4 Tb/s serial optical transport.

Acknowledgments

This work was supported in part by the National Science Foundation (NSF) under Grants CCF-0952711 and ECCS-0725405; through NSF CIAN ERC Center for Integrated Access Network under grant EEC-0812072; and in part by NEC Labs.

#137646 - $15.00 USD Received 3 Nov 2010; revised 23 Dec 2010; accepted 24 Dec 2010; published 6 Jan 2011